Investigation of Er^{3+}-Doped Phosphate Glass for L+ Band Optical Amplification

Xiao Shen, Sheng Chen, Yan Sun, Xin Wang, Wei Wei, and Lili Hu

***Abstract*—In this work, Er^{3+}-doped phosphate glass with good flatness of the emission spectrum of the L+ band was prepared by optimizing the content of BaO. The absorption and emission spectra were measured. Increase of BaO content is conducive to the broadening of the emission spectrum in the L+ band. The dependence of flatness with Raman intensity has been shown by linear fitting. The results show that B31 sample has best flatness of the emission spectrum in the L+ band. It is showed that the largest emission cross-section at 1630 nm is 0.0529×10^{-20} cm^2 and higher than other Er^{3+}-doped phosphate glass. Decay curves of the $^4I_{13/2}$ level were measured and the longest fluorescent lifetime is 10.18 ms and longer than other glass except germinate glass. The broadening of the Er^{3+}-doped phosphate glass spectrum of the L+ band has been achieved successfully, which provides a reference for the material of optical amplifiers.**

***Index Terms*—Optical amplifier, Er^{3+}-doped phosphate glass, L+ band, Raman spectrum.**

I. Introduction

SINCE 1980s, Er^{3+}-doped fibers have been developed as optical amplifiers and been found important applications in optical communications [1]. Quartz-based Er^{3+}-doped fiber amplifiers (EDFA) have been performed for many years [2]. However, the development of new generation communication demands for broadband emissions at wavelength longer than 1610 nm (L+ band) furtherly [3]. Besides, EDFA is difficult to achieve a flat and efficient gain spectrum in L+ band due to the characteristics of Er^{3+} spectrum in silica glass [4].

Instead, among glass hosts, phosphate glass shows many advantages such as mature manufacture technology, high transparency, high doped concentration and large-scale component adjustment [5], [6]. Meanwhile, the spectroscopic properties of Er^{3+} in phosphate glass can be widely adjusted by changing the composition [7]. For instance, the emission line width of rare earth ions in phosphate glass shows great dependence on the composition of alkali and alkaline-earth ions [8], [9]. Therefore, Er^{3+}-doped phosphate glass shows promising potential as host for Er^{3+}-doped fiber amplifiers.

Previous works have investigated the influence of alkali and alkaline-earth ions on the luminescence properties of Nd^{3+} [10], Tm^{3+} [11] and Yb^{3+} [12] in oxide glasses, and the results demonstrated that alkaline-earth ions present more important influence on spectral properties due to their higher ionic field strength. Among alkaline-earth ions, Ba^{2+} in phosphate glass shows an advantage of short stress relaxation time, which is key for synthesis of large-scale bulk glass and optical fibers [9].

There are many studies on the spectral performance of barium ions on phosphate glass. Rouse *et al.* analyzed the influence of the radius and field strength of alkali metal ions on the structure of phosphate glass [13]. Xue *et al.* studied the phosphate glass of the P_2O_5-Li_2O-BaO system [14]. According to Rouse's theory, they believed that substituting Ba^{2+} for Li^+ would reduce the intensity of the symmetric stretching vibration of bridging oxygen, but increase the asymmetric stretching vibration of non-bridging oxygen. Yang listed the spectral parameters of Er^{3+}-doped glass in the (77-x)P_2O_5-8Al_2O_3-(15+x)BaO system [15]. The results show that the introduction of Ba^{2+} can improve the magnification performance of the glass. However, too much Ba^{2+} will destroy the glass structure and reduce the physical and chemical properties of the glass.

In this paper, in order to obtain a multi-component phosphate glass with a flatter spectrum of the L+ band, Er^{3+}-doped phosphate glass with the composition of 8Al_2O_3-22K_2O-xBaO-(69.5–x)P_2O_5- 0.5Er_2O_3 was prepared. The influence of substituting BaO for P_2O_5 on the spectrum and structure of phosphate glass was analyzed systematically. A flatter broadening spectrum of the L+ band of the Er^{3+}-doped phosphate glass has been achieved successfully with a longer lifetime.

II. Experiment

Er^{3+}-doped phosphate glass with a molar composition of 8Al_2O_3-22K_2O-xBaO-(69.5–x)P_2O_5-0.5Er_2O_3, (x = 10, 15, 20, 24, 28 and 31, denoting as B10, B15, B20, B24, B28 and B31, respectively) was prepared by melt quenching technique. The purity of Al $(H_2PO_4)_3$, Al_2O_3, Ba $(H_2PO_4)_2$, KPO_3, Er_2O_3 and P_2O_5 are 99.99%. About 70 g of the batch composition was mixed and melted at 1150 °C for 15 min, then CCl_4 and O_2 were introduced into the melt for 40 min to remove the hydroxyl groups. The glass melt was then poured into a preheated mould

Manuscript received September 1, 2021; revised October 15, 2021; accepted October 26, 2021. Date of publication November 2, 2021; date of current version November 15, 2021. This work was supported in part by the National Natural Science Foundation of China under Grants 62075099 and 62075100, in part by the Natural Science Foundation of Jiangsu Province, China under Grant BK20181391, and in part by the National Key R&D Program of China under Grant 2020YFB1805900. *(Corresponding authors: Xin Wang; Wei Wei).*

Xiao Shen, Sheng Chen, and Wei Wei are with the College of Electronic and Optical Engineering & College of Microelectronics, Nanjing University of Posts and Telecommunications, Nanjing 210023, China (e-mail: shenx@njupt.edu.cn; 929838582@qq.com; weiwei@njupt.edu.cn).

Yan Sun, Xin Wang, and Lili Hu are with the Key Laboratory of Materials for High Power Laser, Shanghai Institute of Optics and Fine Mechanics, Chinese Academy of Sciences,, Shanghai 201800, China (e-mail: albertsunyan@163.com; xinwang@siom.ac.cn; hulili@siom.ac.cn).

Digital Object Identifier 10.1109/JPHOT.2021.3124132

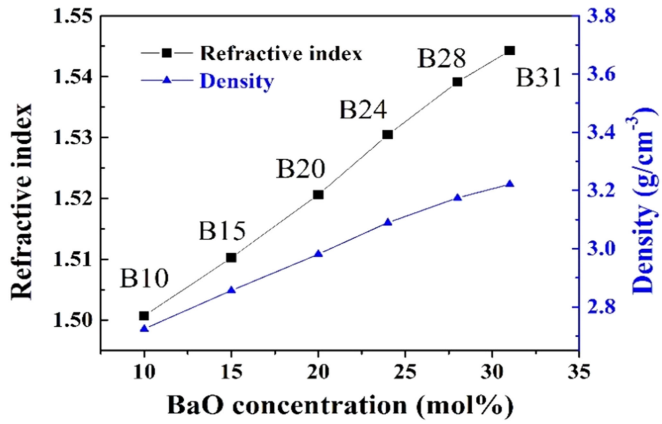

Fig. 1. RI and density of the glass as function of BaO concentration.

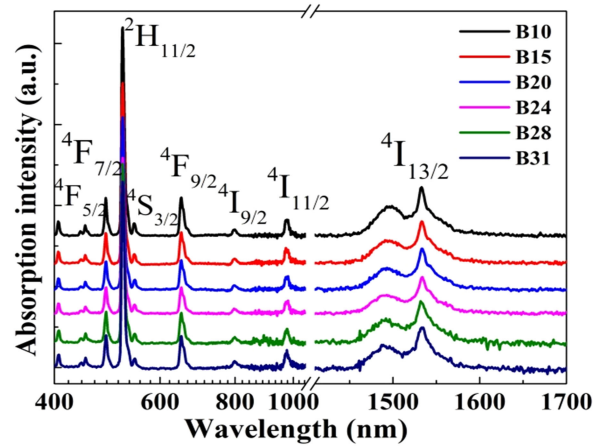

Fig. 2. Absorption spectra of B samples.

and annealed at 460°C for 3 h. All samples were polished for measurements.

Refractive index (RI) was measured by V prism refractometer. Raman spectrum was measured by Renishaw's InVia Raman Microscope. Absorption spectra were measured by Perkin-Elmer's Lambda 950 spectrophotometer. Fluorescence spectra and decay curves were measured with spectrometer model FLSP920 from Edinburgh Company, U.K. Infrared transmission spectra were measured by NEXUS-Fourier-Infrared-Spectrometer from ThermoFisher.

III. Results and Analysis

A. Physical Properties

Fig. 1 shows RI and the density of all phosphate glass samples with different concentration of BaO. RI increases with the increase of BaO concentration. Due to the large ionic radius of Ba^{2+}, the increase of Ba^{2+} concentration will change the symmetry of the electron cloud around oxygen ions, resulting in an increase of molecular refraction and RI of glass.

B. Absorption and Emission Spectra

Fig. 2 shows the absorption spectra of all samples. Each absorption peak corresponds to the transitions from the ground state $^4I_{15/2}$ to the various excited states $^4F_{5/2}$, $^4F_{7/2}$, $^2H_{11/2}$, $^4S_{3/2}$, $^4F_{9/2}$, $^4I_{9/2}$, $^4I_{11/2}$, and $^4I_{13/2}$ of the Er^{3+}, respectively. The location and intensity of the absorption peaks of Er^{3+} in each glass sample are similar.

J-O intensity of samples was calculated as shown in Fig. 3 [16], [17]. According to Tanabe [18], Ω_2 is closely related to the symmetry and order of the glass structure and ligand field, which is more sensitive to the changes in the network modifier. Ω_4 and Ω_6 are related to the covalency of the bond between rare earth ions and oxygen ions, and will decrease with the increase of the covalency. However, compared to Ω_2, the relationship between Ω_4, Ω_6 and the network modifier is less obvious. It can be seen from Fig. 3 that Ω_2 generally shows a decrease trend with the increase of BaO content, which will increase the symmetry of

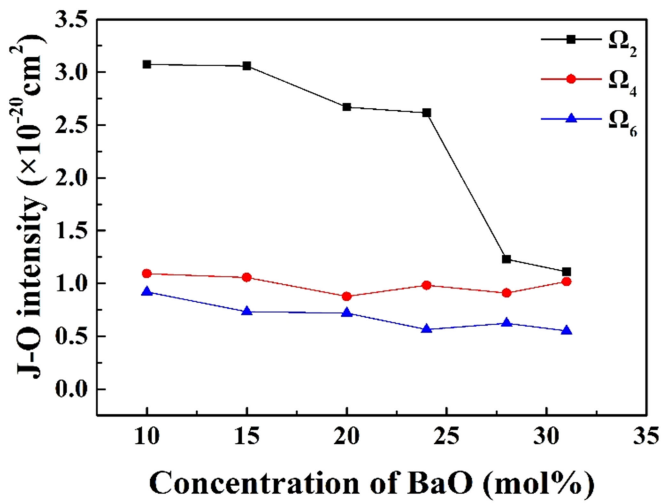

Fig. 3. J-O intensity of Er^{3+} as function of BaO content.

TABLE I
Absorption Coefficients of OH^- in Samples at 3550 cm^{-1}

Samples	B10	B15	B20	B25	B28	B31
α_{OH^-}/cm^{-1}	0.350	0.371	0.235	0.204	0.128	0.132

the ligand around Er^{3+}, because more BaO breaks the chain structure of the phosphate glass.

Because the emission intensity and lifetime of Er^{3+} show great dependence on OH^- group [19]. The transparency spectra were tested and shown in Fig. 4, the absorption coefficient of OH- group can be calculated by

$$\alpha = \ln(T_0/T)/l \tag{1}$$

where l is the thickness of the glass, T_0 is the transmittance of the glass matrix, T is the transmittance of glass at 3550 cm^{-1} [20], and the calculated results are listed in Table I.

The absorption coefficients of B28 and B31 are relatively small, indicating a low OH^- concentration in the samples. Thus,

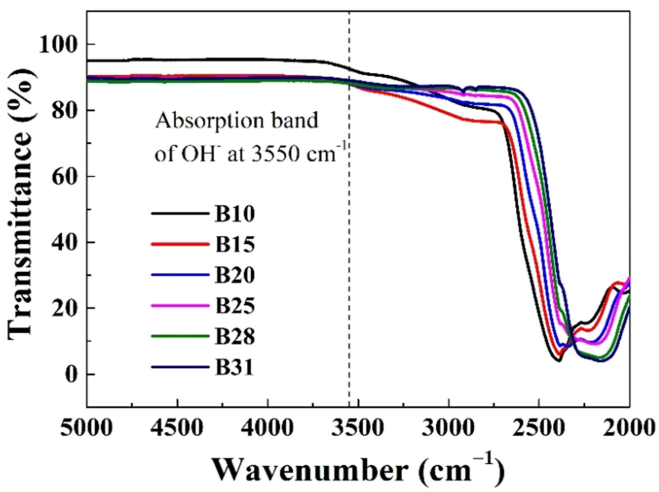

Fig. 4. The infrared transmission spectra of all phosphate glass samples.

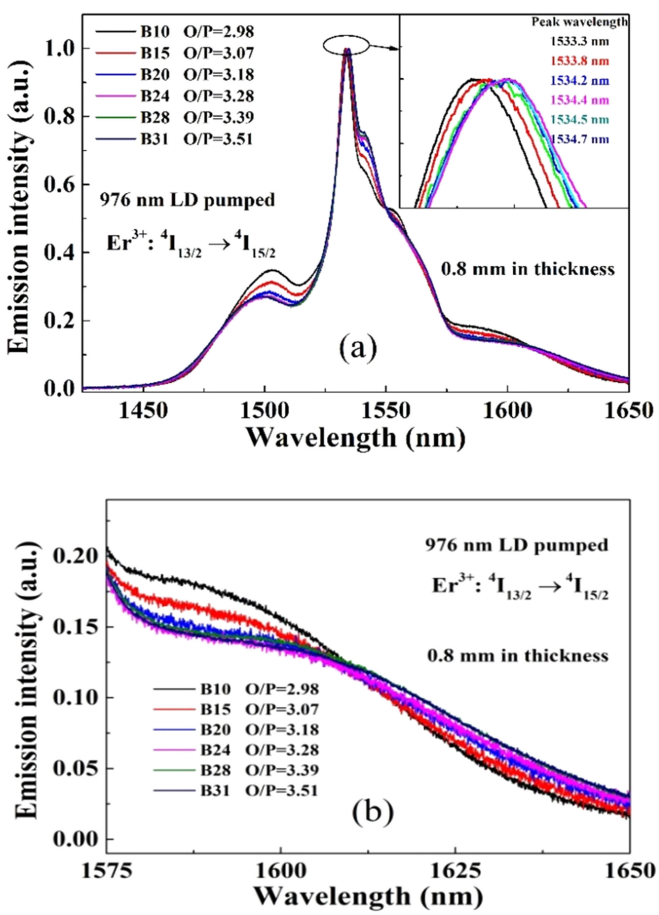

Fig. 5. (a) Emission spectra of Er^{3+}-doped phosphate glass, (b) Emission spectra near 1600nm.

the influence of OH^- on the emission spectrum and lifetime can be ignored.

Fig. 5(a) shows the normalized emission spectra of Er^{3+}-doped phosphate glass from 1450 nm to 1650 nm. The emission peak is around 1534 nm, attributed to the transition from $^4I_{13/2}$ to $^4I_{15/2}$ of Er^{3+}. With the increase of O/P ratio, the intensity become weaker from 1480 nm to 1525 nm and from 1572 nm to 1608 nm, while in the bands of 1534–1550 nm and 1608–1650 nm, the intensity is relatively enhanced. Fig. 5(b) shows the fluorescence spectra of the glass samples around 1600 nm. The spectral shapes of B28 and B31 are very similar and flatter than other samples, which are ideal materials for spectral broadening in L+ band.

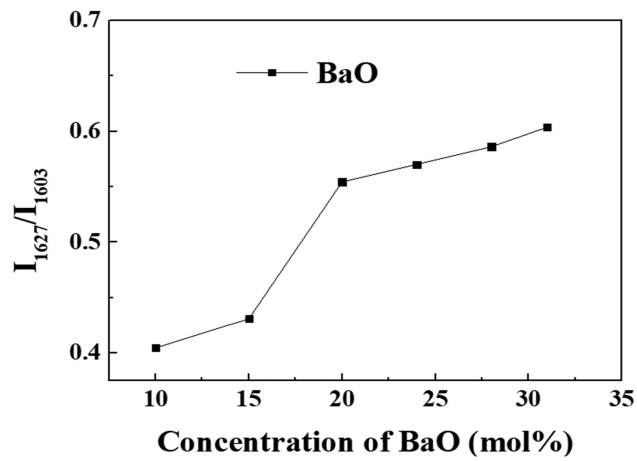

Fig. 6. The value of I_{1627}/I_{1603} varies with the concentration of BaO.

TABLE II
THE VALUES OF I_{1627}/I_{1603} OF VARIOUS GLASS SAMPLES

Glass	B28	B31	Silicate [4]	Tellurite [22]	Phosphate [23]
I_{1627}/I_{1603}	0.5862	0.6039	0.5283	0.2414	0.5051

Fig. 6 shows the relationship between spectral flatness and BaO concentration. It is found that the ratio of the intensity at 1627 nm to the intensity at 1603nm (I_{1627}/I_{1603}) increases with the increase of BaO concentration. The value of I_{1627}/I_{1603} for B20, B24, B28 and B31 are all greater than 0.5, and the maximum value of B31 is 0.6039, which indicates that B31 has the best broadening effect. The I_{1627}/I_{1603} values of some matrix glass samples are given in Table II. It can be seen that the value of I_{1627}/I_{1603} of B31 is the largest, indicating that the spectrum of B31 in L+ band is the flattest.

C. Raman Spectroscopy

Fig. 7 shows the normalized Raman spectra of the samples. It can be seen that there are three strong peaks. Compared to related references, the measured Raman spectra is close to Ref. [24]. According to Ref. [24], the vibration peak near 700 cm^{-1} corresponds to the symmetric stretching vibration of the bridging oxygen of PO^{4-} tetrahedral, the vibration peak near 1180 cm^{-1} is ascribed to the symmetric stretching vibration of the non-bridging oxygen in the Q^2 tetrahedral, while the vibration peak near 1260 cm^{-1} is attributed to the asymmetric stretching vibration of the non-bridging oxygen in the Q^2.

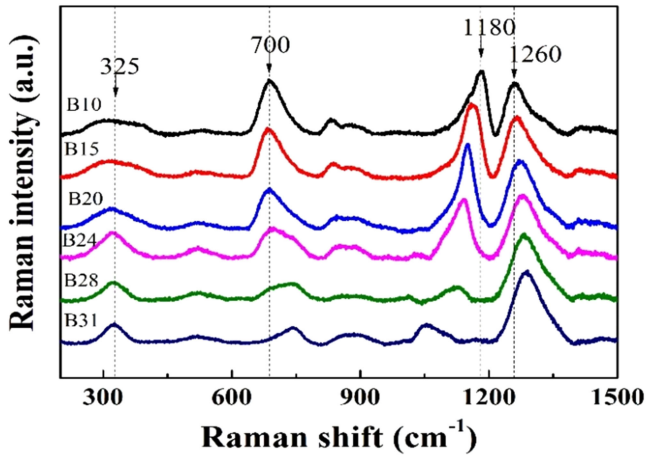

Fig. 7. Raman spectra of the glass samples excited by 633nm light.

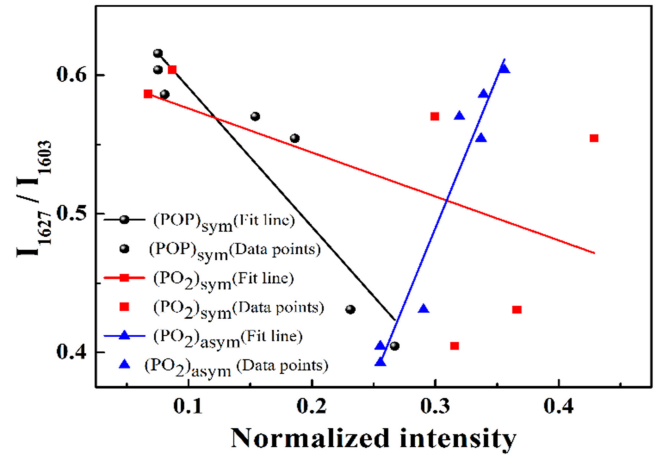

Fig. 8. I_{1627}/I_{1603} values of emission spectra as functions of Raman intensity.

TABLE III
THE RELATIONSHIP BETWEEN THE RAMAN SHIFT OF THE VIBRATION PEAK AND THE BAO CONCENTRATION

Samples	Peak position（cm^{-1}）		
	$(POP)_{sym}$	$(PO_2)_{sym}$	$(PO_2)_{asym}$
B10	685	1185	1256
B15	685	1164	1265
B20	687	1149	1268
B24	698	1142	1281
B28	735	1127	1283
B31	743	1055	1288

By increasing BaO concentration, the vibration peak near 700 cm^{-1} shifts to the short wave direction, the vibration peak near 1180 cm^{-1} shifts to the long wave direction, while the vibration peak near 1260 cm^{-1} shifts towards short wave direction slightly, as showed in Table III. According to reference [7], when the value of O/P rises from 3 to 3.5, the main network structure of phosphate glass will change from Q^2 tetrahedron to Q^1 tetrahedron. Therefore, the $(POP)_{sym}$ vibration peak of Q^2 at 700 cm^{-1} shifts to the $(POP)_{sym}$ vibration peak of Q^1 at 758 cm^{-1}. And the substitution of larger cations for smaller cations will increase the non-bridging oxygen bond angle [13]. As a result, the $(PO_2)_{sym}$ vibration peak moves to the long wavelength direction while the $(PO_2)_{asym}$ vibration moves to the short wavelength direction.

Fig. 8 shows that I_{1627}/I_{1603} values negatively correlated with $(POP)_{sym}$ linearity while positively correlated with $(PO_2)_{asym}$ linearity. However, the fitting results of I_{1627}/I_{1603} values with $(PO_2)_{sym}$ is poor that no obvious dependence between them.

D. Absorption and Emission Cross-Sections

By comparison, the emission cross-section of Er^{3+} in B28 sample is the largest among all the samples and is showed in Fig. 9. The absorption cross-section was calculated by formula (2):

$$\sigma_a(\lambda) = \frac{2.303}{Nl} OD(\lambda) \tag{2}$$

Where $\sigma_a(\lambda)$ is the absorption cross-section, $OD(\lambda)$ is the optical density, N is the concentration of ions and l is the thickness of the sample. According to McCumber theory [25], the emission cross-section $\sigma_e(\lambda)$ can be calculated by formula (3):

$$\sigma_e(\lambda) = \sigma_a(\lambda) \frac{Z_l}{Z_u} \exp\left[\left(\varepsilon - \frac{hc}{\lambda}\right)/kT\right. \tag{3}$$

where, (Z_l/Z_u) is the degeneracy corresponding to the $^4I_{15/2} \rightarrow {}^4I_{13/2}$ transition, h is Planck constant, k is Boltzmann constant, ε is the free energy required to excite a lanthanide ion from the ground state to the previous energy level.

Table IV shows the O/P ratio, Center wavelength, σ_{emi} at center wavelength and σ_{emi} at 1630 nm of different matrix glass. It can be seen that the emission cross-section of B28 is larger than other samples at 1630 nm. On one hand, the increase of Ba^{2+}

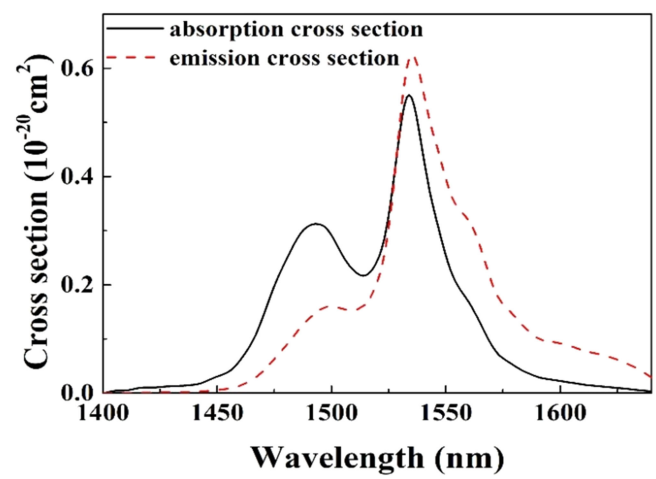

Fig. 9. The absorption and emission cross-sections of B28 sample.

TABLE IV
O/P RATIO, CENTER WAVELENGTH, σ_{EMI} AT CENTER WAVELENGTH, σ_{EMI} AT 1630 nm OF DIFFERENT MATRIX GLASS

Samples	O/P	Center wavelength (nm)	σ_{emi} at center wavelength ($10^{-20}cm^2$)	σ_{emi} at 1630 nm($10^{-20}cm^2$)
B28	3.399	1535	0.6256	0.0529
Phosphate[26]	3.024	1535	0.605	0.0423
Phosphate[27]	3.364	1534	0.746	0.0497
Phosphate[28]	3.202	1535	0.759	0.0075

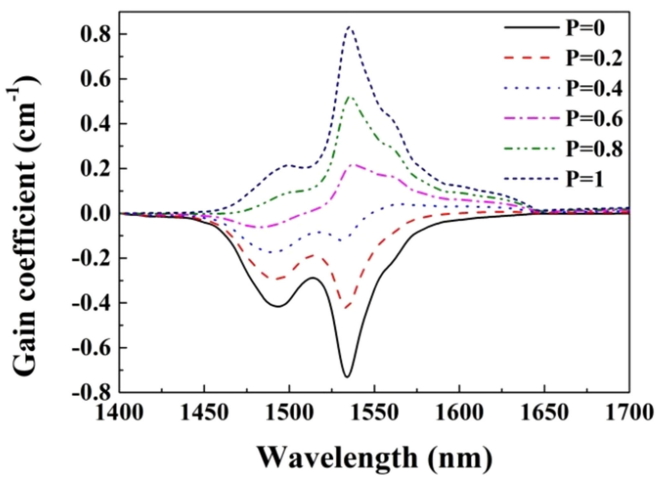

Fig. 10. The calculated net gain coefficients versus wavelengths of B28 glass.

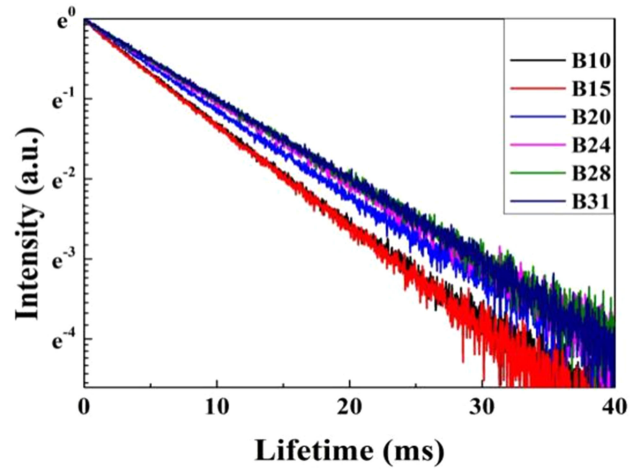

Fig. 11. Decay curves of $^4I_{13/2}$ level of Er^{3+} pumped by a 976nm LD.

TABLE V
FLUORESCENCE LIFETIME OF $^4I_{13/2}$ LEVEL OF ER^{3+}

Samples	τ_{mean}/ms	Samples	τ_{mean}/ms
B10	7.70	Phosphate [26]	0.87
B15	7.65	Germanate [30]	17.17
B20	8.83	Tellurite [31]	3.21
B24	9.75	Sodium phosphate [32]	7.86
B28	10.10	Phosphate [33]	7.6
B31	10.18	Lead silicate [34]	3.7

causes the bridging oxygen to be converted into non-bridging oxygen, which increases the disorder of the local environment around Er^{3+}, on the other hand, the increase in the O/P ratio causes Q_2 group to be converted to Q_1 group, which intensifies the bridge conversion of oxygen to non-bridging oxygen [14]. The higher the degree of disorder in the local environment around rare earth ions, the greater the difference in Stark energy levels and the wider the fluorescence spectrum.

The gain coefficients can be calculated based on the absorption cross-section and emission-cross section of $^4I_{13/2} \leftrightarrow {}^4I_{15/2}$ transition of Er^{3+} by formula (4) [29]:

$$G\ (\lambda) = \mathrm{N}\left[P\sigma_{em}\left(\lambda\right) - \left(1-P\right)\sigma_{abs}\left(\lambda\right)\right] \tag{4}$$

Where, P stands for the population of the upper laser level divided by the total Er^{3+} concentrations N. By calculating the wavelength dependence of the net gain coefficients as a function of population inversion of the upper laser level, we can know the gain property. Fig. 10 shows the calculated gain coefficients versus wavelengths of the $^4I_{13/2} \leftrightarrow {}^4I_{15/2}$ transition of Er^{3+} in the samples. The gain coefficients (1600–1630 nm) will be positive when P is larger than 0.2. Then the samples will have a flat gain bandwidth in the wavelength range of 1600–1630nm, which covers the L+ band of the optical communication window.

E. Fluorescence Lifetime

The decay curves of $^4I_{13/2}$ level of the samples are showed in Fig. 11. Table V shows the fluorescence lifetime of $^4I_{13/2}$ level of all samples and other glasses of different matrices. The lifetime of B31 is the longest (10.18 ms) except for germanate glass. When more P_2O_5 is substituted by BaO, the fluorescence lifetime of Er^{3+} is increased. For more Ba^{2+} content increases the ionic bond composition of Er^{3+} and non-bridging oxygen, and weakens the polarization of non-bridging oxygen on Er^{3+}, which results in decrease of absorption cross-section and increase of fluorescence lifetime of Er^{3+}.

The figure of merit ($\tau_{\exp} \times \sigma_e$) is one of the desirable parameters for lasers and optical amplifiers [35] and should be as large as possible to attain high gain, a longer lifetime permits the required high population inversion to have high and broad amplification, which is essential for Er^{3+}-doped fiber amplifiers.

Fig. 5(b) shows that the emission intensity of B31 is higher than other samples in L+ band, this indicates that the optical amplification capacity is not affected by the signal excited state absorption obviously.

IV. CONCLUSION

In this work, Er^{3+}-doped phosphate glass was prepared and the performance was investigated. Different samples were obtained by substituting BaO for P_2O_5. It can be seen from the

value of I_{1627}/I_{1603} that B31 sample has the best flatness of emission spectrum of Er^{3+} in the L+ band. The absorption and emission cross-sections of B28 glass sample were calculated, and it is noticed that the emission cross-section ($0.0529 \times 10^{-20} cm^2$) of B28 at 1630 nm is greater than other phosphate glass, which is more conducive to obtain a large gain coefficient. Decay curves show that the lifetime of the $^4I_{13/2}$ level of Er^{3+} increases with increase of BaO, and the longest fluorescence lifetime reaches 10.18 ms. The data in this paper show that B28 and B31 samples are both suitable for optical amplifiers in L+ band.

References

[1] M. Z. Amin, K. K. Qureshi, and M. M. Hossain, "Doping radius effects on an erbium-doped fiber amplifier," *Chin. Opt. Lett.*, vol. 17, no. 1, pp. 14–19, 2019.

[2] S. D. Alaruri, "Single stage C-band erbium-doped fiber amplifier (EDFA) development and performance evaluation," *Int. J. Meas. Technol. Instrum. Eng.*, vol. 72, pp. 41–49, 2018.

[3] A. A. Al-Azzawi, A. A. Almukhtar, A. Dhar, M. C. Paul, and S. W. Harun, "Gain-flattened hybrid EDFA operating in C + L band with parallel pumping distribution technique," *IET Optoelectron.*, vol. 14, no. 6, pp. 447–451, 2020.

[4] Y. Jiao, M. Guo, R. Wang, C. Shao, and L. Hu, "Influence of Al/Er ratio on the optical properties and structures of Er3+ /Al3+ co-doped silica glasses," *J. Appl. Phys.*, vol. 129, no. 5, 2021, Art. no. 053104.

[5] M. Mortier, A. Monteville, G. Patriarche, G. Mazé, and F. Auzel, "New progresses in transparent rare-earth doped glass-ceramics," *Opt. Mater.*, vol. 16, no. 1/2, pp. 255–267, 2001.

[6] D. Pugliese *et al.*, "Concentration quenching in an Er-doped phosphate glass for compact optical lasers and amplifiers," *J. Alloys Compounds*, vol. 657: pp. 678–683, 2016.

[7] R. K. Brow, R. J. Kirkpatrick, and G. L. Turner, "Nature of alumina in phosphate glass: II, structure of Sodium Alurninophosphate glass," *J. Amer. Ceram. Soc.*, vol. 76, no. 4, pp. 919–928, 1993.

[8] D. Murthy, A. M. Babu, B. C. Jamalaiah, L. R. Moorthy, and J. H. Jeong, "Photoluminescence properties of Er^{3+}-doped alkaline earth titanium phosphate glasses," *Opt. Mater.*, vol. 491, no. 1, pp. 349–353, 2010.

[9] N. Kitamura, T. Hayashido, N. Matsushita, K. Fukumi, and H. Kozuka, "Viscoelastic behavior of alkali and alkaline earth aluminophosphate glasses," *J. Non Cryst. Solids*, 2021, Art. no. 120441.

[10] J. S. Hayden, Y. T. Hayden, and J. H. Campbell, "Effect of composition on the thermal, mechanical, and optical properties of phosphate laser glasses," in *Proc. SPIE Int. Soc. Opt. Eng.*, vol. 1277, 1990, pp. 121–139.

[11] W. Xin, S. Fan, K. Li, Z. Lei, S. Wang, and L. Hu, "Compositional dependence of the 1.8 μm emission properties of Tm^{3+} ions in silicate glass," *J. Appl. Phys.*, vol. 112, no. 10, 2012, Art. no. 103521.

[12] Y. Sun, X. Wang, M. Liao, L. Hu, and T. Wang, "Compositional dependence of Stark splitting and spectroscopic properties in Yb^{3+}-doped lead silicate glasses," *J. Non Cryst. Solids*, vol. 532, 2020, Art. no. 119890.

[13] G. B. Rouse, Jr., P J. Miller, and W. M. Risen Jr., "Mixed alkali glass spectra and structure," *J. Non Cryst. Solids*, vol. 28, no. 2, pp. 193–207, 1978.

[14] G. Xue and G. Wang, "Effects on glass structure of BaO substitution in Li_2O–P_2O_5 glasses," *J. Wuhan Univ. Technol.*, vol. 2, pp. 145–152, 1989.

[15] G. Yang, Z. Deng, B. Yin, Z. Feng, and Z. Jiang, "Effect of alkaline earth matal oxide on spectroscopic properties of erbium-doped phosphate glasses," *J. Chin. Ceram. Soc.*, vol. 32, no. 8, pp. 954–958, 2004.

[16] B. R. Judd, "Optical absorption intensities of rare-earth ions," *Phys. Rev.*, vol. 127, no. 3, pp. 750–761, 1962.

[17] S. G. Ofelt, "Intensities of crystal spectra of rare-earth ions," *J. Chem. Phys.*, vol. 37, no. 3, pp. 511–520, 1962.

[18] S. Tanabe, "Optical transitions of rare earth ions for amplifiers: How the local structure works in glass," *J. Non Cryst. Solids*, vol. 259, no. 1, pp. 1–9, 1999.

[19] Y. Yan, A. J. Faber, and H. D. Waal, "Luminescence quenching by OH groups in highly Er-doped phosphate glasses," *J. Non Cryst. Solids*, vol. 181, no. 3, pp. 283–290, 1995.

[20] Q. Nie *et al.*, "Effect of hydroxyl groups on Er^{3+} doped Bi_2O_3-B_2O_3-SiO_2 glasses," *J. Phys. Chem. Solids*, vol. 68, no. 4, pp. 477–481, 2007.

[21] R. Francini, F. Giovenale, U. M. Grassano, P. Laporta, and S. Taccheo, "Spectroscopy of Er and Er–Yb-doped phosphate glasses," *Opt. Mater.*, vol. 13, no. 4. pp. 417–425, 2000.

[22] M. S. Sajnaa, S. Thomas, C. Jayakrishnan, C. Joseph, P. R. Biju, and N. V. Unnikrishnan, "NIR emission studies and dielectric properties of Er^{3+}-doped multicomponent tellurite glasses," *Spectrochimica Acta A. Mol Biomol. Spectrosc.*, vol. 161, pp. 130–137, 2016.

[23] M. Caetano, J. Filho, R. F. Moraes, A. A. Andrade, and N. O. Dantas, "Effect of the OH groups on spectroscopic parameters of the Er^{3+}-Doped glasses," *Braz. J. Phys.*, vol. 50, no. 4, pp. 1–9, 2020.

[24] A. Mogu-Milankovi, A. Gajovi, A. Anti, and D. Day, "Structure of sodium phosphate glasses containing Al_2O_3 and/or Fe_2O_3. Part I," *J. Non Cryst. Solids*, vol. 289, no. 1-3, pp. 204–213, 2001.

[25] D. E. McCumber, "Theory of phonon-terminated optical masers," *Phys. Rev.*, vol. 134, no. 2A, pp. A299–A306, 1964.

[26] K. Linganna *et al.*, "1.53 m luminescence properties of Er^{3+}-doped K–Sr–Al phosphate glasses," *Ceramics Int.*, vol. 41, no. 4, pp. 5765–5771, 2015.

[27] T. Maheswari, B. Ch, K. Linganna, S. Ju, W. T. Han, and C. K. Jayasankar, "Structural and spectroscopic properties of γ-ray irradiated Er^{3+} -doped lead phosphate glasses," *J. Lumin.*, vol. 203, pp. 322–330, 2018.

[28] I. Soltani, S. Hraiech, K. Horchani-Naifer, H. Elhouichet, and M. Férid, "Effect of silver nanoparticles on spectroscopic properties of Er^{3+} doped phosphate glass," *Opt. Mater.*, vol. 46, pp. 454–460, 2015.

[29] X. Zou and H. Toratani, "Spectroscopic properties and energy transfers in Tm3+ singly- and Tm3+Ho3+ doubly-doped glasses," *J. Non Cryst. Solids*, vol. 195, no. 1/2, pp. 113–124, 1996.

[30] R. Wang *et al.*, "Effect of optical basicity on broadband infrared fluorescence in erbium-doped germanate glasses," *J. Alloys Compounds*, vol. 513, pp. 339–342, 2012.

[31] H. Lin *et al.*, "Near-infrared emissions with widely different widths in two kinds of Er^{3+}-doped oxide glasses with high refractive indices and low phonon energies," *J. Lumin.*, vol. 124, no. 1, pp. 167–172, 2007.

[32] A. A. Reddy, S. S. Babu, K. Pradeesh, C. J. Otton, and G. V. Prakash, "Optical properties of highly Er^{3+}-Doped sodium–aluminium–phosphate glasses for broadband 1.5 μm emission," *J. Alloys Compounds*, vol. 509, no. 9, pp. 4047–4052, 2011.

[33] R. Lachheb, A. Herrmann, A. A. Assadi, K. Damak, C. Rüssel, and R. Maalej, "Judd Ofelt analysis and experimental spectroscopic study of erbium doped phosphate glasses," *J. Lumin.*, vol. 201, pp. 245–254, 2018.

[34] W. A. Pisarski, J. Pisarska, R. Lisiecki, and W. Ryba-Romanowski, "Erbium-doped lead silicate glass for near-infrared emission and temperature-dependent up-conversion applications," *Opto-Electron. Rev.*, vol. 25, no. 3, pp. 238–241, 2017.

[35] K. Linganna, K. Suresh, S. Ju, W.-T. Han, C. K. Jayasankar, and V. Venkatramu, "Optical properties of Er3+-doped K-Ca-Al fluorophosphate glasses for optical amplification at 1.53 μm," *Opt. Mater. Exp.*, vol. 5, no. 8, pp. 1689–1703, 2015.